Eur. J. Med. Chem. 34 (1999) 919–937

Original article

β_1- and β_2-Adrenoceptor antagonist activity of a series of *para*-substituted *N*-isopropylphenoxypropanolamines

Simon N. Louis*, Tracy L. Nero, Dimitri Iakovidis, Felicia M. Colagrande, Graham P. Jackman, William J. Louis

Clinical Pharmacology and Therapeutics Unit, The University of Melbourne, Department of Medicine, Austin and Repatriation Medical Centre Heidelberg 3084, Victoria, Australia

(Received 8 July 1998; revised 14 April 1999; accepted 20 May 1999)

Abstract – To further explore the structure-activity relationships of β-adrenoceptor (β-AR) antagonists, a series of 25 *para*-substituted *N*-isopropylphenoxy-propanolamines were synthesised, nine of which are new compounds. All have been examined for their ability to antagonise β_1-ARs in rat atria and β_2-ARs in rat trachea. Substitution in the *para*-position of the phenyl ring is thought to confer β_3-specificity and the selectivity of these compounds for the β_1-AR ranges from 1.5–234. None of the compounds tested were selective for the β_2-AR. Of the 25 compounds studied, 22 had reasonable ($pA_2 > 7$) potencies for the rat β_1-AR. Only compound **1** displayed reasonable ($pA_2 > 7$) potency for the rat β_2-AR. Twenty two compounds were used as the training set for comparative molecular field analysis (CoMFA) of antagonist potency (pA_2) at the rat β_1- and β_2-ARs. The inclusion of a number of additional physical characteristics improved the QSAR analysis over models derived solely using the CoMFA electrostatic and steric fields. The final models predicted the β_1- and β_2-AR potency of the compounds in the training set with high accuracy ($r^2 = 0.93$ and 0.86 respectively). The final β_1-AR model predicted the β_1-potencies of two out of the three test compounds, not included in the training set, with residual pA_2 values < –0.14, whereas the test compounds were not as well predicted by our final β_2-AR model (residual pA_2 values < –0.38). © 1999 Éditions scientifiques et médicales Elsevier SAS

comparative molecular field analysis / rat β-adrenoceptors / β-adrenoceptor antagonists / *N*-isopropylphenoxypropanolamines / quantitative structure activity relationships

1. Introduction

β-Adrenoceptors (β-ARs) are members of the large family of G-protein coupled receptors [1–4]. It has been established so far that there are at least three β-AR subtypes, designated the β_1-, β_2- and β_3-ARs [5–7]. *N*-Isopropylphenoxypropanolamine (*figure 1*, R = H) is considered to be a non-selective β-AR antagonist. Many structure-activity studies in the past have focused upon the *N*-isopropylphenoxypropanolamine core structure with substitutions in the *ortho* and/or *meta* positions [8, 9]. However, the effects of *para*-substituents upon the β-blocking activity of this core structure have received less attention [10–12]. Previous work by us [10, 13] and others [11, 12, 14, 15] has established that high β_1-AR selectivity and potency can be achieved by *para*-substitution of the phenyl ring and/or appropriate substitution of the phenoxypropanolamine amino group (e.g. -ethyl-3-(4-hydroxyphenyl)urea [13]).

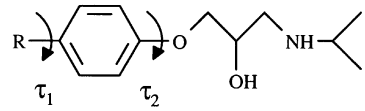

Figure 1. General structure of *para*-substituted *N*-isopropyl-phenoxypropanolamines. The torsion angles τ_1 and τ_2 define the conformation of the *para*-substituent and the oxypropanolamine side-chains respectively in relation to the phenyl ring, for example when $\tau_1 = 0$ the *para*-substituent is planar to the phenyl ring.

*Correspondence and reprints

Abbreviations: Aryloxypropanolamine, AOPA; β-adrenoceptors, β-ARs; comparative molecular field analysis, CoMFA; ESP phenyl ring charge, ESP; flexibility of the para-substituent, flexibility; length of the para-substituent, length; optimal number of components, ONC; partial least squares, PLS; standard error, SE.

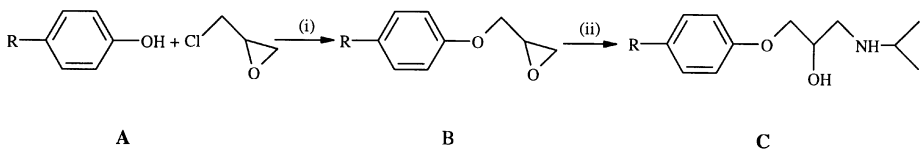

Figure 2. General procedure for preparing *N*-isopropylphenoxypropanolamines. Reagents: (i) aqueous KOH, ETOH; (ii) isopropylamine, ETOH.

To further examine the effect of *para*-substitution upon both β_1- and β_2-AR selectivity and potency, we have synthesised a series of *para*-substituted *N*-isopropylphenoxypropanolamines. Nine of these compounds are new (**6**, **7**, **9**, **10**, **15**, **16**, **18**, **20** and **22**), that is to say that a chemical abstracts structure database search indicated that these compounds have not been previously reported. Eleven previously reported compounds (**1**, **2**, **3**, **4**, **5**, **8**, **12**, **14**, **19**, **23** and **25**) and five commercially available compounds (**11** (metoprolol), **13** (H 87/07), **17** (betaxolol), **21** (RO 31-1118) and **24** (cicloprolol)) have also been synthesised and included in the study in order to obtain comparative pharmacological data in the rat. All of these compounds have been examined in our laboratory for their ability to antagonise β_1-ARs in rat atria and β_2-ARs in rat trachea, which are well established as sources of the β_1- and β_2-AR subtypes respectively [16]. The synthesis and structure-activity relationships, using comparative molecular field analysis (CoMFA), of these *para*-substituted *N*-isopropylphenoxypropanolamines are presented here.

2. Chemistry

All compounds were prepared as their racemic mixtures by the general procedure shown in *figure 2*. It has been established for simple phenoxypropanolamines that the S-isomer is the active isomer, with little β-AR activity residing with the R-isomer [17–19]. Resolution of the racemate into the individual isomers or stereospecific synthesis was therefore not carried out. The corresponding phenols **A** reacted under aqueous alkaline conditions with epichlorohydrin to produce the epoxides **B**. After isolation, the crude epoxides **B** were allowed to react with isopropylamine overnight to furnish the desired compounds **C**.

Compounds **1**, **2**, **3**, **4**, **5**, **8**, **11** (metoprolol), **12**, **13** (H 87/07), **14**, **17** (betaxolol), **22**, **21** (RO 31-1118), **23**, **24** (cicloprolol) and **25**, have been previously reported and were prepared following literature procedures [20–33]. All intermediates and final compounds had virtually identical physical and chemical data with those reported.

The precursor phenols of compounds **6, 10, 15** and **16** were prepared by reacting bromoethane, n-bromopropane, 4-cyclohexylethyl bromide and 4-fluorophenylethyl bromide with 4-benzyloxyphenol, thus producing the benzyl ethers **D** which were subsequently hydrogenated giving the desired phenols **E** (4-ethoxyphenol), **F** (4-n-propoxyphenol), **G** (4-cyclohexylethoxyphenol) and **H** (4-fluorophenethoxyphenol) as shown in *figure 3*.

The precursor phenols of compounds **18**, **20** and **22** were prepared by the sequence of reactions shown in

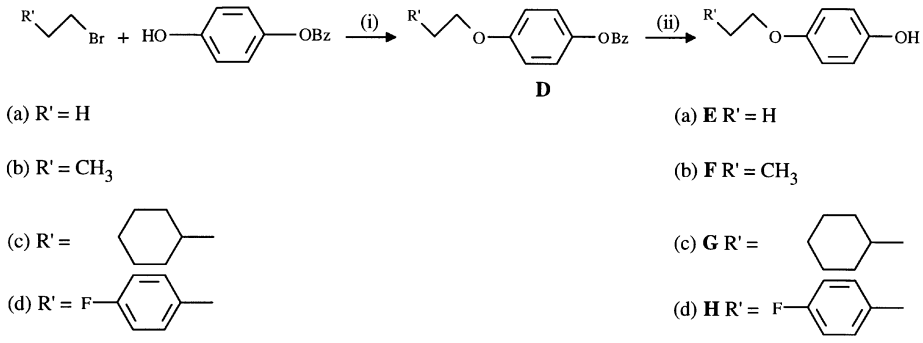

Figure 3. Reagents: (i) K_2CO_3/NaI, anhydrous acetone; (ii) H_2, 10% Pd/C.

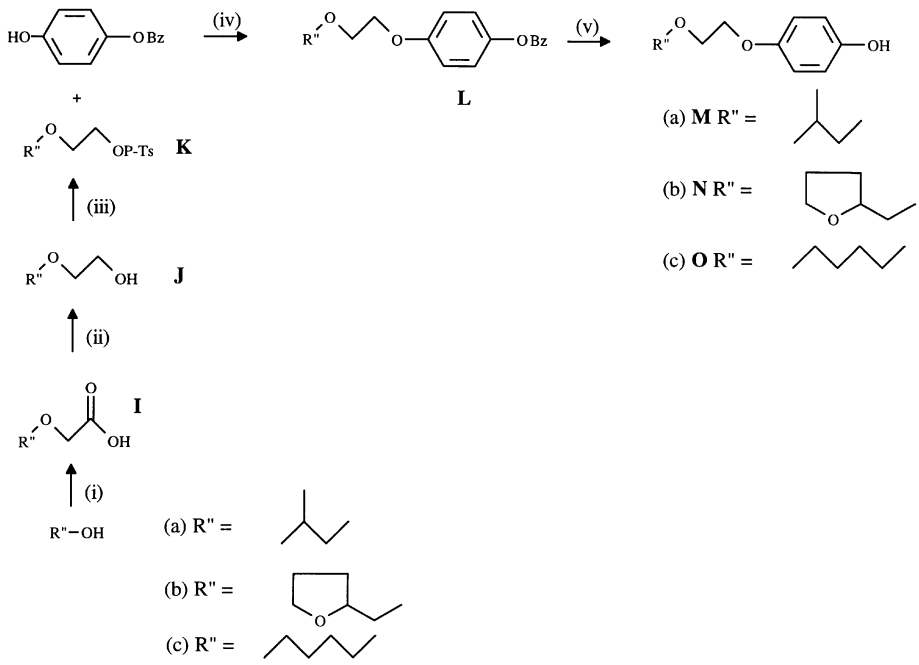

Figure 4. Reagents: (i) $ClCH_2COOH$, NaH, DMF; (ii) $LiAlH_4$, THF; (iii) pTsCl, pyridine; (iv) NaH, DMF; (v) H_2, 10% Pd/C.

figure 4. The corresponding alcohols 2-methylpropane-1-ol, 2-hydroxymethyltetrahydrofuran and n-pentane-1-ol reacted with chloroacetic acid to furnish the corresponding alkoxy acetic acids **I**. These were reduced to their corresponding alkoxy-ethanols **J** whose tosylates **K** reacted with 4-benzyloxyphenol, to produce the benzyl ethers **L** which were subsequently hydrogenated giving the desired phenols **M**, **N** and **O**.

The precursor phenol of compound **7** was prepared by the reactions shown in *figure 5* [34, 35]. Phenyl-n-butanoate reacted with aluminium chloride to furnish a mixture of regioisomers P (2- and 4-hydroxypropiophenone), of which 4-hydroxypropiophenone, after isolation, was reduced with sodium amalgam to produce the desired phenol **Q**.

The precursor phenol of compound **9** was prepared according to the reactions shown in *figure 6*. Ethyl-4-hydroxyphenyl propionate was benzylated to produce the ether **R**, which was subsequently reduced to give the protected alcohol **S**. Hydrogenation of **S** produced the desired phenol **T**.

The above mentioned phenols were then used to produce compounds **6**, **7**, **9**, **10**, **15**, **16**, **18**, **20** and **22** following the general procedure shown in *figure 2*. The general physical data for these compounds are given in *table I*.

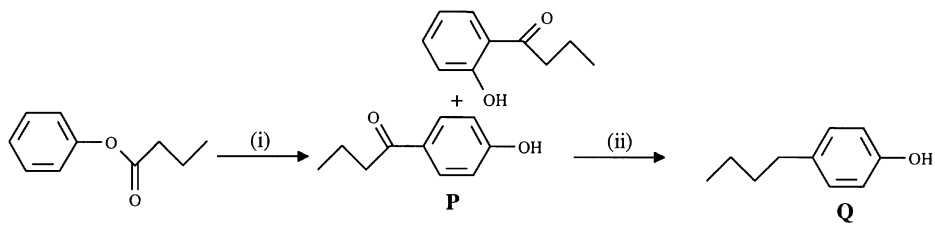

Figure 5. Reagents: (i) anhydrous $AlCl_3$; (ii) Zn-Hg, MeOH, HCl.

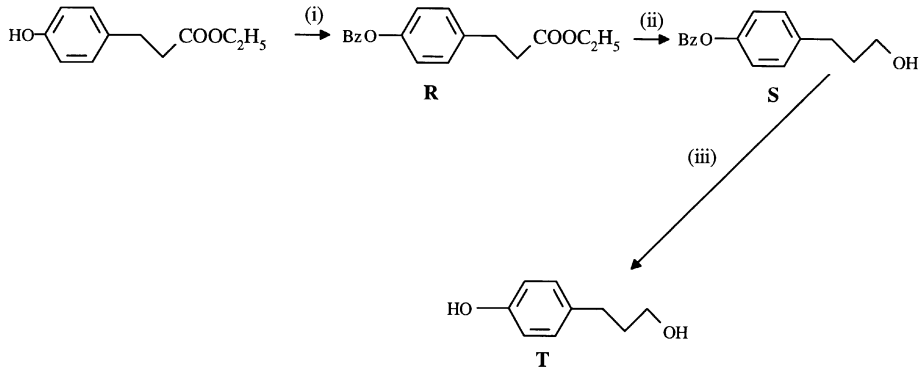

Figure 6. Reagents: (i) BzBr, K_2CO_3, NaI, anhydrous acetone; (ii) $LiALH_4$, THF; (iii) H_2, 10% Pd/C.

3. Pharmacology

All compounds were evaluated for their ability to antagonise β_1- and β_2-ARs in rat atria and tracheal rings respectively. Cumulative concentration-response curves were obtained in each preparation as described by Van Rossum [36] and curves were fitted by computer analysis according to the method of Zabrowsky et al. [37] using the sigmoidal fit function of the Origin graphics package [38]. The antagonist potencies, or pA_2 values, were calculated using equation 1 [39] and represent the mean ± SE from 4–9 individual experiments. The β-AR antagonist potencies and the subtype selectivity are given in *table II*.

$$pA_2 = -\log\left(\frac{[\text{antagonist}]}{\text{dose ratio} - 1}\right) \quad (1)$$

where the dose ratio =

$$\frac{[\text{(-)-isoprenaline}] \text{ at } EC_{50} \text{ in the presence of antagonist}}{[\text{(-)-isoprenaline}] \text{ at } EC_{50} \text{ in the absence of antagonist}}$$

Table I. Physical data for compounds **6**, **7**, **9**, **10**, **15**, **16**, **18**, **20** and **22**.

Compound	Yield (from phenol)	M.p. (°C) HCl salt[a]	Formula[b]
6	3.66 g (63.4 %)	87.5–88.5	$C_{14}H_{23}NO_3$.HCl
7	4.35 g (72.1 %)	70.5–73.0	$C_{16}H_{27}NO_2$.HCl
9	2.41 g (39.7 %)	68.5–71.5	$C_{15}H_{25}NO_3$.HCl
10	3.56 g (58.6 %)	116.5–119.0	$C_{15}H_{25}NO_3$.HCl
15	4.91 g (66.3 %)	131.0–133.0	$C_{20}H_{33}NO_3$.HCl
16	11.71 g (61.4 %)	136.0–138.0	$C_{20}H_{26}FNO_3$.HCl
18	4.00 g (55.3 %)	89.5–91.3	$C_{18}H_{31}NO_4$.HCl
20	3.59 g (48.4 %)	165.5–167.0	$C_{11}H_{31}NO_5$.HCl
22	3.90g (52.1 %)	77.0–79.0	$C_{19}H_{33}NO_4$.HCl

[a]Ethanol-ether was the solvent system used for recrystallisation. [b]Empirical formula; elemental analyses were carried out for the nine compounds shown and were within 0.4% per element.

Table II. Antagonist activity, subtype selectivity, flexibility of para-substituent, π, ESP phenyl ring charge at 90° and 0° and length of the para-substituent for the compounds examined in this study.

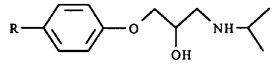

Compound	R Group	β_1-AR[a] pA_2	β_2-AR[b] pA_2	β_1-AR selectivity[c]	Flexibility[d]	π[e]	ESP phenyl ring charge at 90° (e)	ESP phenyl ring charge at 0° (e)	Length[f] (Å)
Training Compounds									
1	—H	8.09 ± 0.14	7.47 ± 0.14	4.2	0	0.00	–0.83	–0.83	0.00
2	—NH_2	6.60 ± 0.18	6.43 ± 0.17	1.5	0	–0.86	–0.67	–0.67	1.41
3	—CH_3	7.13 ± 0.04	6.47 ± 0.11	4.6	0	0.47	–0.71	–0.71	1.53
4	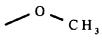	6.58 ± 0.19	6.34 ± 0.09	1.7	1	–0.04	–0.68	–0.72	2.30
5		7.41 ± 0.13	6.56 ± 0.18	7.1	2	1.37	–0.76	–0.72	3.84
6		7.08 ± 0.27	5.94 ± 0.16	14	2	0.36	–0.71	–0.74	3.61
7		7.49 ± 0.26	6.23 ± 0.23	18	3	1.82	–0.72	–0.68	5.00
8		7.38 ± 0.19	5.39 ± 0.16	98	3	–0.09	–0.75	–0.69	5.06
9		7.13 ± 0.10	6.58 ± 0.34	3.5	3	0.06	–0.72	–0.69	4.86
10	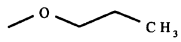	7.16 ± 0.14	5.72 ± 0.38	28	3	0.84	–0.68	–0.72	4.79
11	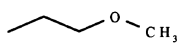	7.60 ± 0.17	6.43 ± 0.13	15	3	0.11	–0.72	–0.69	4.86
12	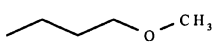	7.98 ± 0.21	6.77 ± 0.28	16	4	0.57	–0.74	–0.70	6.14
13	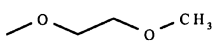	7.37 ± 0.09	5.97 ± 0.19	25	4	–0.13	–0.68	–0.72	5.91
14	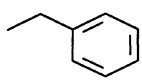	6.67 ± 0.09	5.36 ± 0.18	20	2	2.06	–0.68	–0.69	5.08
15	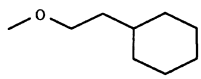	7.65 ± 0.12	5.93 ± 0.23	52	4	2.57	–0.66	–0.70	6.45
16	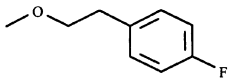	8.01 ± 0.12	5.64 ± 0.12	234	4	2.13	–0.70	–0.73	8.72
17	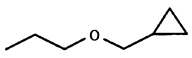	8.06 ± 0.15	6.38 ± 0.13	48	5	0.96	–0.73	–0.70	7.39

Table II. Continued

Compound	R Group	β_1-AR[a] pA_2	β_2-AR[b] pA_2	β_1-AR selectivity[c]	Flexibility[d]	π[e]	ESP phenyl ring charge at 90° (e)	ESP phenyl ring charge at 0° (e)	Length[f] (Å)
Training Compounds									
18	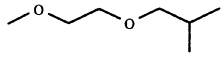	7.75 ± 0.22	5.69 ± 0.20	115	6	1.13	–0.73	–0.70	8.54
19	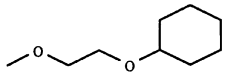	7.61 ± 0.15	5.40 ± 0.18	162	5	1.76	–0.72	–0.69	9.51
20	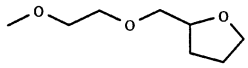	7.74 ± 0.09	5.49 ± 0.27	178	6	0.32	–0.69	–0.73	9.36
21	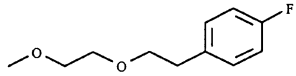	7.98 ± 0.21	5.68 ± 0.10	200	7	2.05	–0.72	–0.73	12.4
22	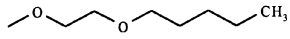	8.04 ± 0.23	5.80 ± 0.24	174	8	1.66	–0.72	–0.72	10.8
Test Compounds									
23		7.22 ± 0.08	6.47 ± 0.17	5.6	1	0.92	–0.77	–0.75	2.50
24	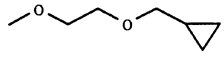	7.73 ± 0.07	5.44 ± 0.10	195	6	0.72	–0.73	–0.70	8.59
25	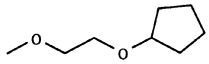	8.04 ± 0.30	5.81 ± 0.25	170	5	1.31	–0.74	–0.70	8.36

[a]β_1-AR antagonist pA_2 value ± SEM determined in isolated spontaneously beating rat atria. [b]β_2-AR antagonist pA_2 value ± SEM determined in rat tracheal chain preparation. [c]Selectivity = antilog (pA_2 β_1-AR – pA_2 β_2-AR). [d]Flexibility was defined as the number of fully rotatable non-H bonds in the *para*-substituent. [e]π was logP of the compound in question minus logP of compound **1**, logP was calculated using PrologP. [f]Length was defined as the distance between the *para*-carbon atom of the phenyl ring and the most distant non-H atom.

4. Results and discussion

4.1. Isolated tissue preparations

Functional potencies of compounds **1**–**25** for inhibiting (-)-isoprenaline-induced: (i) β_1-AR mediated chronotropic effects in spontaneously beating rat atria; and (ii) β_2-AR mediated relaxation of rat tracheal chain previously contracted with 1 μM carbachol are listed in *table II*. The unsubstituted reference compound **1** had a high potency at both the β_1-AR (pA_2 = 8.09) and β_2-AR (pA_2 = 7.47). *Para*-substitution reduced the potency of the compounds for both β_1- and β_2-ARs (compounds **2**–**11**, **13**–**15**, **18**, **19**, **20**, **23** and **24**; *table II*), except for compounds **12**, **16**, **17**, **21**, **22** and **25** (β_1-AR pA_2s = 7.98–8.06) which had similar β_1-AR potencies to the unsubstituted compound **1**. Compound **12** (β_2-AR pA_2 = 6.77) was the most potent of the *para*-substituted compounds at inhibiting rat β_2-ARs (c.f. reference compound **1**, pA_2 = 7.47).

Overall, the compounds had higher potencies for the β_1-AR than the β_2-AR, with the β_1/β_2 selectivities ranging from 1.5–234. Compounds **1**, **2**, **3**, **4**, **9** and **23**, however, were at the lower end of the selectivity scale and are considered to be non-selective in the rat.

The animal species used in this study to determine both the β_1- and β_2-AR functional potency of the compounds was the rat. Previously published β_1-AR antagonist functional potency, or activity data has been obtained from both the rat and guinea-pig [30, 40], whereas the guinea-pig is the commonly used animal species for published β_2-AR antagonist activity [30, 40]. By using the rat as the source for both β_1- and β_2-ARs, any

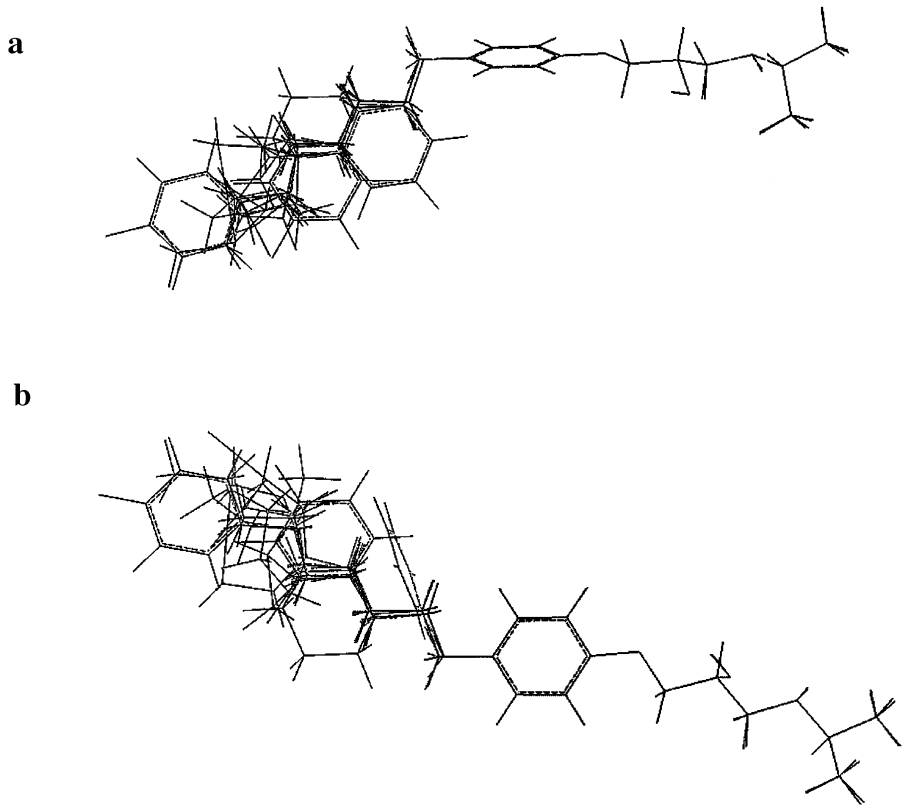

Figure 7. (a) Structural alignment of the training set of compounds (compounds **1–22**) when $\tau_1 = 90°$. **(b)** Structural alignment of the training set of compounds when $\tau_1 = 0°$.

interspecies differences between the receptor subtypes was removed.

4.2. Alignment of molecules

The alignment of the compounds is the most important feature of CoMFA analysis [41]. It has been proposed that AOPA type compounds interact with β-ARs via a three point pharmacophore consisting of the β-hydroxyl group, the amino group and an electron rich moiety which is usually a phenyl ring [42, 43] and more recent site-directed mutagenesis studies support this hypothesis [44–47]. If we assume the compounds all act via the same mechanisms, then these common points of interaction must superimpose and hence we have assumed that the AOPA core structure remains fixed for all compounds in our conformational analysis.

Previous studies within our laboratory [10] examined two conformations of each molecule ie. $\tau_1 = 90°$ or 0°. In the present study we have examined the effect of these values of τ_1 on our CoMFA analysis. *Figure 7a* displays the superimposition of the compounds when $\tau_1 = 90°$ and *figure 7b* when $\tau_1 = 0°$.

4.3. CoMFA analysis for antagonist potency at the rat β_1-AR

The CoMFA (SYBYL version 6.40) results for antagonist potency at rat β_1-ARs for the twenty-two compounds in the training set are given in *table III*. A range of column filtering values were used (1.0–16.0 kcal/mol). Column filtering omits from the analysis columns, lattice points whose variance is less than the specified value (SYBYL). Partial least squares analysis (PLS) of the data identified that when τ_1 was set to 90° (*figure 1*) and the default CoMFA settings were used, which included both steric and electrostatic fields, the highest cross validated r^2 (q^2) value was obtained when column filtering was set to 4.0 kcal/mol ($q^2 = 0.24$; optimum number of components (ONC) = 4; *table III*). When $\tau_1 = 0°$, q^2 was maximised when column filtering was set at 5.0 kcal/mol ($q^2 = 0.38$ and ONC = 2; *table III*).

Table III. CoMFA results for rat β_1-ARs (n = 22).

Analysis variables	τ_1	Column filtering	q^2	ONC	SE
CoMFA	90°	4	0.244	4	0.461
CoMFA, flexibility[a]	90°	4	0.527	3	0.354
CoMFA, ESP[b,c]	**90°**	**13**	**0.747**	**10**	**0.332**
CoMFA, length[d]	90°	4	0.322	6	0.465
CoMFA, π	90°	4	0.186	5	0.493
CoMFA, flexibility, ESP	90°	9	0.686	4	0.331
CoMFA, flexibility, length	90°	4	0.375	4	0.419
CoMFA, flexibility, π	90°	4	0.398	4	0.411
CoMFA, ESP, length	90°	13	0.672	10	0.358
CoMFA, ESP, π	90°	13	0.638	10	0.388
CoMFA, length, π	90°	4	0.247	5	0.474
CoMFA, flexibility, ESP, length	90°	9	0.655	4	0.311
CoMFA, flexibility, ESP, π	90°	10	0.632	5	0.332
CoMFA, flexibility, length, π	90°	4	0.259	4	0.457
CoMFA, ESP, length, π	90°	5	0.636	7	0.352
CoMFA, flexibility, ESP, length, π	90°	9	0.610	5	0.341
CoMFA	0°	5	0.384	2	0.394
CoMFA, flexibility[a]	0°	5	0.592	2	0.320
CoMFA, ESP[b]	0°	5	0.604	4	0.334
CoMFA, length[c]	0°	5	0.524	2	0.346
CoMFA, π	0°	5	0.553	2	0.335
CoMFA, flexibility, ESP	0°	5	0.657	2	0.294
CoMFA, flexibility, length	0°	5	0.571	2	0.328
CoMFA, flexibility, π	0°	5	0.515	3	0.359
CoMFA, ESP, length	0°	5	0.618	2	0.310
CoMFA, ESP, π	0°	5	0.601	4	0.335
CoMFA, length, π	0°	5	0.407	3	0.397
CoMFA, flexibility, ESP, length	0°	5	0.635	2	0.303
CoMFA, flexibility, ESP, π	0°	2	0.599	6	0.357
CoMFA, flexibility, length, π	0°	5	0.482	3	0.371
CoMFA, ESP, length, π	0°	5	0.563	4	0.351
CoMFA, flexibility, ESP, length, π	0°	5	0.564	6	0.373

[a]Flexibility of the *para*-substituent. [b]Bold indicates the options used for the final model. [c]ESP phenyl ring charge. [d]Length of the *para*-substituent.

In addition to the PLS analysis of the CoMFA data, several other physical parameters of the compounds were determined and included in further CoMFA analysis. These parameters included the flexibility, length and π of the *para*-substituent and the ESP phenyl ring charge (*table II*). The flexibility of the *para*-substituent (flexibility) was determined by assigning an integer value for the number of torsion angles which affected the conformation of the substituent. The term 'ESP phenyl ring charge' (ESP) was defined in this study as the sum of the six phenyl ring carbon atom esp charges. The phenyl ring charges of all the compounds studied (*table II*) were calculated using the AM1 Hamiltonian within MOPAC (version 6.0), specifying the key words 'ESP', 'PRECISE' and 'NOMM'. The length of the *para*-substituent (length) was defined as the distance between the *para*-carbon of the phenyl ring and the most distant non-H atom, hence the *para*-substituent length of compound **1** is zero (*table II*). The π value of the *para*-substituent was defined as the logP of the compound minus the logP of compound **1**, logP having been calculated using Pallas PrologP (version 1.1). When these additional parameters were included with CoMFA they generally improved q^2. For instance, when $\tau_1 = 90°$ a combination of the CoMFA fields and ESP gave the highest q^2 (q^2 = 0.769; ONC = 11; SE = 0.332; *table III*), and when $\tau_1 = 0°$ a combination of the CoMFA fields, ESP and flexibility maximised q^2 (q^2 = 0.657; ONC = 2; SE = 0.29; *table III*). The former model was selected for further analysis as it possessed the highest q^2 of any of the β_1-AR models examined (*table III*).

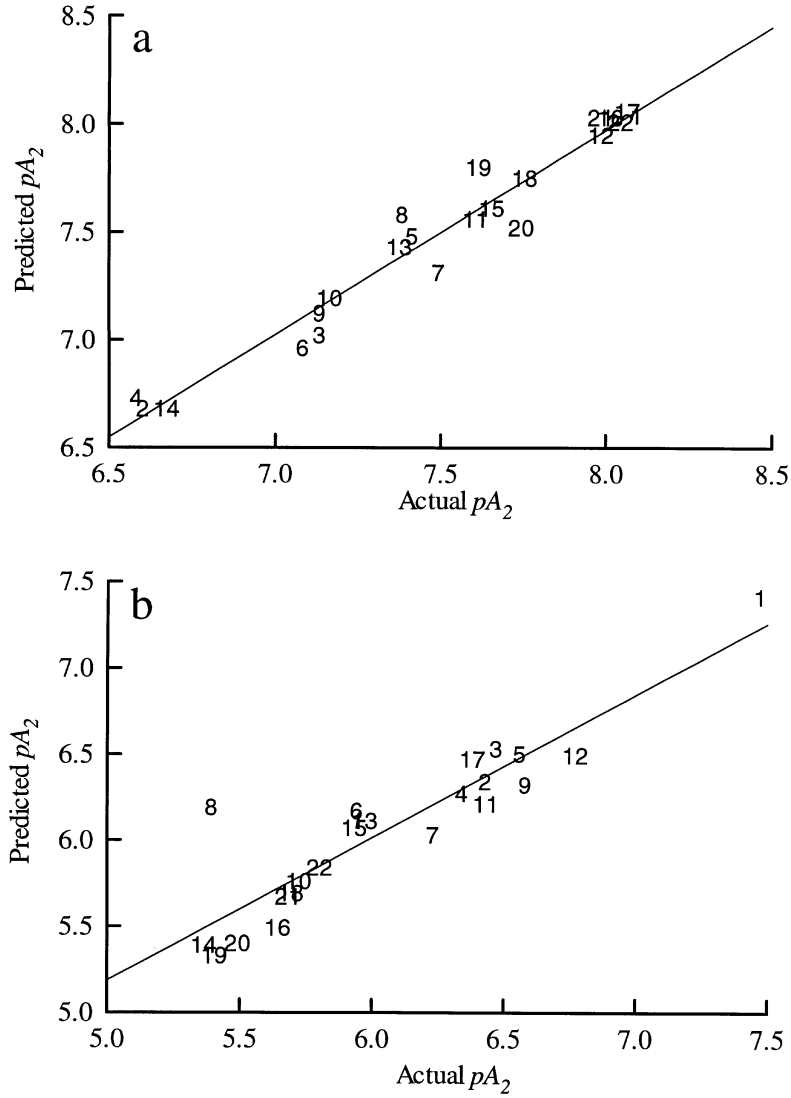

Figure 8. **(a)** Plot of the actual β_1-AR pA_2 verses the predicted β_1-AR pA_2 compounds in *table II* (n = 22) using the final model, non cross validated, and an optimum number of components of 4. **(b)** Plot of the actual β_2-AR pA_2 verses the predicted β_2-AR pA_2 compounds in *table II* (n = 22) using the final model, non cross validated, and an optimum number of components of 4.

The final model, without cross validation, was obtained using the default CoMFA options, 10 ONC and 13 kcal/mol column filtering, $\tau_1 = 90^o$, including ESP. This model had an r^2 value of 0.95, a standard error (SE) of 0.15 and an F (11, 10) of 21.47. The regression equation for ESP, taken from the PLS output file, was:

$$\beta_1\text{-}pA_2 = 0.995–8.49\ ESP$$

The relative contributions of the components were: steric, 0.88; electrostatic, 0.00; and ESP, 0.12. *Figure 8a* displays the relationship between calculated and measured pA_2 values for the non-cross validated analysis and residual values are given in *table IV*.

4.4. CoMFA analysis for antagonist potency at the rat β_2-AR

Similarly, the default CoMFA settings and a range of column filtering values (1.0–16.0 kcal/mol) were used when analysing the β_2-AR data. When $\tau_1 = 90^o$ the highest q^2 value was obtained when column filtering was

Table IV. CoMFA Experimental, calculated and residual activities of the training set of compounds for β_1-ARs.

Compound	Experimental	Calculated	Residual
1	8.09	8.04	0.05
2	6.60	6.68	–0.08
3	7.13	7.02	0.11
4	6.58	6.73	–0.15
5	7.41	7.48	–0.07
6	7.08	6.96	0.12
7	7.49	7.31	0.18
8	7.38	7.58	–0.20
9	7.13	7.12	0.01
10	7.16	7.19	–0.03
11	7.60	7.56	0.04
12	7.98	7.95	0.03
13	7.37	7.43	–0.06
14	6.67	6.68	–0.01
15	7.65	7.61	0.04
16	8.01	8.03	–0.02
17	8.06	8.06	0.00
18	7.75	7.75	0.00
19	7.61	7.80	–0.19
20	7.74	7.52	0.22
21	7.98	8.03	0.05
22	8.04	8.01	0.03

set to 4 kcal/mol (q^2 = 0.50; ONC = 5; *table V*). When τ_1 = 0°, q^2 was maximised when column filtering was set to 5 kcal/mol (q^2 = 0.45; ONC = 2; *table V*). When the additional parameters were included in the analysis the highest q^2 occurred when τ_1 = 90°, column filtering was set at 6 kcal/mol and both flexibility and ESP were considered in addition to the steric and electrostatic fields generated within CoMFA (q^2 = 0.60; ONC = 4; SE = 0.38).

The final model, without cross-validation, for the β_2-AR was obtained using 4 ONC, column filtering set at 6 kcal/mol and included flexibility and ESP. This model had an r^2 value of 0.83, SE of 0.25 and an F (4, 17) of 20.71. The regression equation for flexibility and ESP was:

$$\beta_2\text{-}pA_2 = 2.05 + 0.07 \text{ flexibility} – 6.46 \text{ ESP}.$$

The relative contributions of the components were: steric, 0.73; electrostatic, 0.00; flexibility, 0.11; and ESP, 0.161. *Figure 8b* displays the relationship between the calculated and measured pA_2 values for the cross validated analysis and residual values are given in *table VI*.

It is important to note that by using the column filtering values to maximise the q^2 for the β_1- and β_2-AR models (column filtering = 13 and 6 kcal/mol, respectively) it effectively removes the electrostatic field parameter from the CoMFA analysis. For both models this occurs at column filtering values of 5 kcal/mol when τ_1 = 90° and 6 kcal/mol when τ_1 = 0°.

4.5. Comparison of contour maps

Figures 9A and *9B* show compound **16** binding within the steric contour maps for the final β_1- and β_2–AR models. The experimental data suggests that *para*-substitution decreases antagonist potency at both β_1- and β_2-ARs. However, the contour maps, of the β_1- and β_2-AR pharmacophores display important differences, the most striking of which appears to be a bulk preferring pocket in the β_1-AR which can be accessed by long flexible *para*-substituents. Compounds that access this pocket have their β_1-AR potency restored and the longer the substituent the greater the restoration of their activity, compare the activity of compounds **4**, **13** and **22**. Compounds with shorter bulky substituents, like compound **14** cannot access this pocket and have low β_1-AR potencies. The β_2-AR, on the other hand, seems far more sterically restricted than the β_1-AR in the *para*-position. For instance, the addition of the short bulky substituent of compound **14** reduces the β_1-AR potency by 1.42 log units when compared to the base compound, whereas this substituent reduces β_2-AR potency by 2.11 log units.

Using compound **16** as an example the differences between the two steric maps can be clearly illustrated. In the β_1-AR model (*figure 9A*), the *para*-substituent of compound **16** does not impinge on the sterically restricted region (ie. yellow region), however, the terminal fluorophenyl ring is embedded in the bulk preferring pocket (i.e. green region) and hence the β_1-potency is almost restored to that of compound **1** (*table II*). By contrast, the *para*-substituent of compound **16** is clearly embedded in the sterically restricted region of the β_2-AR model (*figure 9B*) and hence this compound has a much lower β_2-pA_2 than compound **1** (*table II*).

4.6. Predictive abilities of the CoMFA models

The potencies of three test compounds (*table VII*), not in the training set, were predicted at rat β_1- and β_2-ARs using the final models and the predict property function in the QSAR package of SYBYL (version 6.40). For the β_1-AR the predicted potencies for two of the compounds were in close agreement with those obtained experimentally (residuals < 0.15). For the β_2-AR, however, all three compounds were relatively poorly predicted (residuals –0.25 to –0.38) suggesting that our CoMFA model of the β_2-AR is not sufficiently resolved.

Table V. CoMFA results for rat β_2-ARs (n = 22).

Analysis variables	τ_1	Column filtering	q^2	ONC	SE
CoMFA	90°	4	0.501	5	0.434
CoMFA, flexibility[a]	90°	4	0.574	4	0.389
CoMFA, ESP[b]	90°	6	0.586	4	0.383
CoMFA, length[c]	90°	4	0.499	6	0.449
CoMFA, π	90°	4	0.364	4	0.475
CoMFA, flexibility, ESP[d]	**90°**	**6**	**0.602**	**4**	**0.376**
CoMFA, flexibility, length	90°	4	0.498	4	0.422
CoMFA, flexibility, π	90°	4	0.387	5	0.481
CoMFA, ESP, length	90°	4	0.575	5	0.400
CoMFA, ESP, π	90°	5	0.454	3	0.428
CoMFA, length, π	90°	4	0.284	3	0.490
CoMFA, flexibility, ESP, length	90°	5	0.587	4	0.383
CoMFA, flexibility, ESP, π	90°	7	0.430	5	0.464
CoMFA, flexibility, length, π	90°	4	0.372	3	0.459
CoMFA, ESP, length, π	90°	12	0.473	2	0.409
CoMFA, flexibility, ESP, length, π	90°	12	0.455	2	0.416
CoMFA	0°	5	0.445	2	0.420
CoMFA, flexibility[a]	0°	5	0.462	4	0.437
CoMFA, ESP[b]	0°	2	0.453	5	0.454
CoMFA, length[c]	0°	5	0.463	4	0.437
CoMFA, π	0°	5	0.351	5	0.495
CoMFA, flexibility, ESP	0°	2	0.454	5	0.454
CoMFA, flexibility, length	0°	5	0.479	4	0.430
CoMFA, flexibility, π	0°	7	0.538	9	0.482
CoMFA, ESP, length	0°	2	0.459	5	0.452
CoMFA, ESP, π	0°	1	0.386	6	0.497
CoMFA, length, π	0°	7	0.494	9	0.505
CoMFA, flexibility, ESP, length	0°	2	0.491	5	0.438
CoMFA, flexibility, ESP, π	0°	1	0.387	6	0.497
CoMFA, flexibility, length, π	0°	1	0.440	10	0.555
CoMFA, ESP, length, π	0°	1	0.451	6	0.470
CoMFA, flexibility, ESP, length, π	0°	1	0.475	6	0.460

[a]Flexibility of the *para*-substituent. [b]ESP phenyl ring charge. [c]Length of the *para*-substituent. [d]Bold indicates the options used for the final model.

5. Discussion

The aim of this study was to determine the optimal structural requirements of *para*-substituted *N*-isopropyl-phenoxypropanolamines to maximise antagonist potency and selectivity for β_1-ARs. The study also provides information on the extent to which the CoMFA derived models of the rat β_1- and β_2-ARs differed for a series of *para*-substituted β-AR antagonists. Although *para*-substitution generally reduced antagonist potency at both β_1- and β_2-ARs, differences did exist between the two models. For both models, steric factors were the most important (0.88 for β_1- and 0.73 for β_2-ARs). The β_1-AR also possesses a pocket which prefers bulky substituents. Long flexible compounds that accessed this region had their β_1-AR potency restored which is consistent with our previous work [10] that suggested a hydrophobic binding site existed that was accessible to long *para*-substituents containing a ring system. Our data, however, suggests that although the pocket accommodated large, hydrophobic substituents, eg. compounds **15**, **16** and **21**, it will also accept large, less hydrophobic substituents such as compounds **17**, **24** and **25** and long flexible carbon chains like compound **22**. The important characteristic is that the substituent is able to access this pocket, for example, shorter hydrophobic compounds that cannot reach the pocket, like compound **14**, encounter steric hindrance and have low β_1-potency.

In addition, a number of other physical characteristics of the compounds seemed to influence their potency at β_1- and β_2-ARs. For both β_1- and β_2-ARs, ESP was negatively correlated with potency suggesting that the more negative the phenyl ring charge the higher the β_1- or

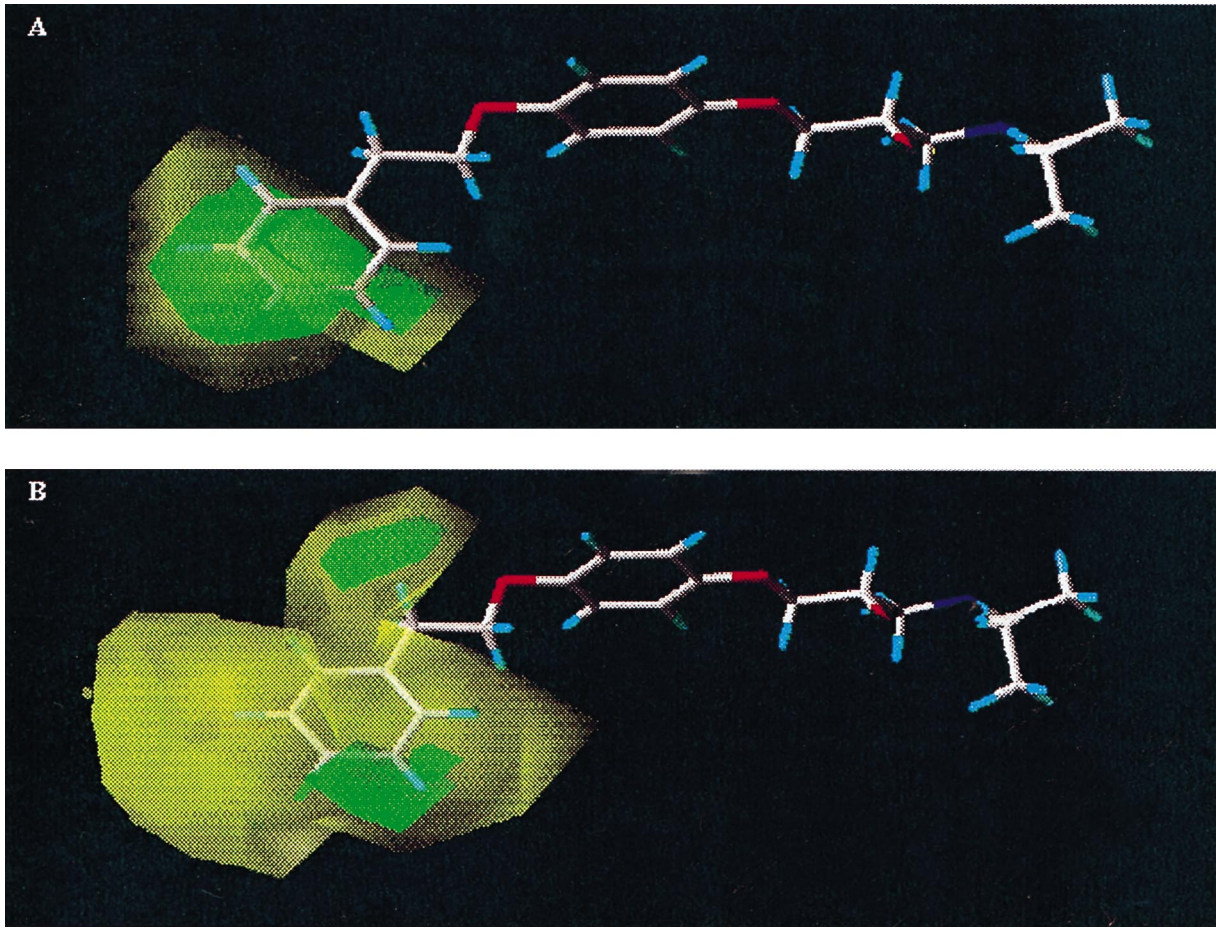

Figure 9. (A) CoMFA contour map of the final model of the β_1-AR with compound **16** embedded. Green areas show favoured areas where increasing bulk is associated with higher potency, yellow areas where increasing bulk is associated with lower potency and blue areas where positive charge is associated with higher potency. **(B)** CoMFA contour map of the final model of the β_2-AR with compound **16** embedded.

β_2-AR potency which supports the hypothesis of previous workers that an electron rich moiety is an essential pharmacophoric element for binding to β-ARs [42, 43]. In addition, flexibility was positively correlated with β_2-AR potency and this may be related to the ability of more flexible *para*-substituents to avoid sterically restricted regions in the β_2-AR.

Unfortunately, our synthetic program was designed to examine β_1-AR potency and hence only compound **1** had high potency ($pA_2 > 7.0$) at the rat β_2-AR and higher affinity compounds are required before we can confidently predict the structure of the β_2-AR pharmacophore. We can say, however, that the β_2-AR appears to be very sterically restricted around the *para*-position of the phenyl ring of AOPA antagonists.

On the whole, the potency of the training set of compounds were predicted better by the β_1-AR model ($r_2 = 0.95$; residuals $< \pm 0.22$) than the β_2-AR model ($r_2 = 0.83$; residuals $< \pm 0.80$). In particular, the potency of compound **8** was over estimated for the β_2-AR. This may have been due to the existence of a negative charge preferring region in the region of the positively charged amine in the *para*-substituent. This, however, was not identified by CoMFA perhaps due to the small number of compounds examined that possess this characteristic. It is of interest that the OH-group of compound **9**, which has an electronegative nature, has significantly higher β_2-AR potency than compound **8** and slightly higher activity than the uncharged substituent of compound **7** (*table II*), therefore, this region requires further study.

Table VI. CoMFA Actual, calculated and residual activities of the training set of compounds for β_2-ARs.

Compound	Actual	Calculated	Residual
1	7.47	7.41	0.06
2	6.43	6.34	0.09
3	6.47	6.53	–0.06
4	6.34	6.27	0.07
5	6.56	6.50	0.06
6	5.94	6.17	–0.23
7	6.23	6.03	0.20
8	5.39	6.19	–0.80
9	6.58	6.32	0.26
10	5.72	5.76	–0.04
11	6.43	6.21	0.22
12	6.77	6.49	0.28
13	5.97	6.11	–0.14
14	5.36	5.39	–0.03
15	5.93	6.07	–0.14
16	5.64	5.49	0.15
17	6.38	6.47	–0.09
18	5.69	5.69	0.00
19	5.40	5.33	0.07
20	5.49	5.40	0.09
21	5.68	5.67	0.01
22	5.80	5.84	–0.04

The two CoMFA models expand the results of earlier studies [10–15] that high β_1-selectivity and potency can be achieved by *para*-substitution of the phenyl ring. For *para*-substituted *N*-isopropylphenoxy-propanolamines it appears at least two factors contribute to β_1-potency. These are the ability of the *para*-substituent to access a bulk preferring pocket and the phenyl ring charge. The latter is negatively correlated with potency.

6. Experimental section

6.1. Chemistry

6.1.1. General

Melting points were determined using a manual Gallenkamp electrothermal apparatus (range 0–200 °C) in glass capillary tubes and are uncorrected. IR spectra were recorded on a Perkin-Elmer FT IR 1600. NMR spectra were recorded on a Varian Associates EM 360 spectrometer and are expressed in δ using TMS (tetramethyl silane) as reference. Mass spectra were recorded on a Finnigan 4000 series GC/MS Mass spectrometer or a Thermo Instruments GCQ Mass spectrometer using methane gas as the ionising medium for CI (chemical ionisation spectra). All spectra were consistent with the assigned structures. Where analyses are indicated only by the symbols of the elements, results obtained were within ± 0.4% of the theoretical values. Descriptions of the synthetic procedures for preparing compounds **6**, **7**, **9**, **10**, **15**, **16**, **18**, **20** and **22** are outlined below. No attempts were made to maximise yields.

Table VII. Comparison of predicted and experimentally determined potencies at rat β_1- and β_2-ARs for the test compounds.

Compound	Receptor	Actual	Predicted	Residual
23	β_1-	7.22	7.52	–0.30
24	β_1-	7.73	7.88	0.15
25	β_1-	8.04	7.94	0.10
23	β_2-	6.47	6.85	–0.38
24	β_2-	5.44	5.80	–0.36
25	β_2-	5.81	6.06	–0.25

6.1.2. Materials

Phenol, 4-methylphenol, 4-ethylphenol, 4-methoxyphenol, 4-benzyloxyphenol, 4-fluorophenol, p-cresol, 4-aminophenol, 4-fluorophenethyl bromide, 2-cyclohexyl-1-bromoethane, 2-(4-benzyloxyphenyl)-1-ethanol, benzyl bromide, 4-toluene sulfonylchloride, phenyl-n-butanoate, ethylchloroformate, bromoethane, iodomethane, 2-hydroxymethyl tetrahydrofuran, 2-methyl-propane-1-ol, n-pentanol, isobutanol, cyclopentanol, cyclohexanol, chloroacetic acid, ethyl-4-hydroxyphenyl propionate, lithium aluminium hydride and dimethyl formamide (DMF) were purchased from Aldrich Chemicals. Sodium hydride and isopropylamine were obtained from Fluka Chemicals. Anhydrous aluminium chloride was obtained from Merck. Inorganic reagents were supplied by Ajax Chemicals. Analytical grade solvents, including carbon disulphide, were purchased from Rhone Poulenc Australia. (-)-Isoprenaline and carbachol were obtained from Sigma. Silica plates (5 × 10 cm, Silica F_{254}) were purchased from Merck. Silica for column chromatography (100 Å, 50 mm) was supplied by Amicon Inc., MA 01923, USA.

6.1.3. General procedure 1 for the synthesis of 1-phenoxy-2,3-epoxypropanes (**B**)

The phenol **A** (20 mmol), KOH (1.23 g, 22 mmol) and epichlorohydrin (5.55 g, 60 mmol) in EtOH (60 mL) were stirred overnight at room temperature. The reaction mixture was evaporated to dryness and the residue was partitioned between ether (or EtOAc) and water. The organic layer was washed with aqueous NaOH (5%), followed by a water wash and then dried over Na_2SO_4. After the solvent was evaporated, the residue was freed from excess epichlorohydrin under vacuum and used

without further purification. All epoxides were homogenous by TLC (silica, eluent dichloromethane).

6.1.4. General procedure 2 for preparing N-isopropyl-phenoxypropanolamines (**C**)

The crude 1-phenoxy-2,3-epoxypropane **B** (20 mmol) and isopropylamine (100 mmol, 5 molar excess) in EtOH (60 mL) were stirred overnight at room temperature. The reaction mixture was evaporated to dryness and the residue was dissolved in ethanol and then treated with excess ethereal HCl. The crude precipitate was recrystallised from a suitable solvent or purified by column chromatography (silica, eluent: CH_2Cl_2/MeOH/NH_4OH 28%, 90:9:1).

6.1.5. 4-Ethoxyphenol (**E**)

Ethyl bromide (6.0 g, 55 mmol), 4-benzyloxyphenol (10.11 g, 50 mmol), anhydrous K_2CO_3 (8.29 g, 60 mmol) and NaI (0.5 g) were stirred and refluxed in anhydrous acetone (250 mL) for 48 h. The solvent was evaporated and the residue was partitioned between dichloromethane and water. The organic layer was washed with water and dried over anhydrous $MgSO_4$. The solvent was evaporated and the residual 4-ethoxyphenylbenzylether **D** (R = H) was recrystallised from EtOH. Yield = 8.2 g, 81.5%; m.p. = 64–66 °C; MS m/e 229 (M + 1); ^{1}H-NMR ($CDCl_3$) δ 1.58 (3H, t), 4.15 (2H, q), 5.17 (2H, s), 7.06 (5H, s), 7.58 (4H, s).

The ether **D** (R = H) (7.2 g, 36 mmol) in EtOH (200 mL) was hydrogenated over 10% Pd/C (0.1 g) at room temperature and atmospheric pressure. When hydrogen absorption ceased, the reaction mixture was filtered and evaporated to dryness. The product **E** was recrystallised from EtOH. Yield = 4.26 g, 87.0%; m.p. = 64.5–65.5 °C; MS m/e 139 (M + 1); ^{1}H-NMR ($CDCl_3$) δ 1.61 (3H, t), 4.19 (2H, q), 5.63 (1H, s), 6.93 (4H, s).

6.1.6. 1-(4-Ethoxyphenoxy)-3-isopropylamino-2-propanol (**6**)

Prepared from **E** according to the general procedures 1 and 2, chromatographed and isolated as the hydrochloride. Yield = 3.66 g, 63.4%; m.p. = 87.5–88.5 °C; MS m/e 254 (M + 1); ^{1}H-NMR (CD_3OD) δ 1.33 (6H, d), 1.62 (3H, t), 2.16–3.23 (6H, bm), 4.23 (2H, q), 7.10 (4H, s). Anal. ($C_{14}H_{23}NO_3$.HCl) C, H, Cl, N.

6.1.7. 4-n-Butylphenol (**Q**)

Phenyl-n-butanoate (82.0 g, 500 mmol) was added into a stirred suspension of aluminium chloride (75 g) in carbon disulphide (80 mL) to furnish, after work-up, a mixture of 2- and 4-hydroxyphenylpropiophenones (butyrophenones) (64.5 g, 78.6%) which were separated by repeated fractional distillation. The desired 4-hydroxyphenyl propiophenone **P** was obtained in overall 33.4% yield (27.4 g) and had the following physical data: b.p. = 148–150 °C (11.5 mm Hg); MS m/e 165 (M + 1); ^{1}H-NMR (CD_3OD) δ 1.14 (3H, t), 2.39–2.82 (2H, m), 3.62–3.98 (2H, m), 6.97 (5H, dd, the phenolic hydrogen is hiding under the aromatic protons).

Reduction of **P** (27.0 g, 166 mmol) was achieved by its portion wise addition into freshly prepared sodium amalgam (68.0 g of powdered Zn and 5.03 g of $HgCl_2$ in 650 mL of methanol and 320 mL of concentrated HCl), evaporation of methanol, isolation and chromatography on silica (eluent CH_2Cl_2:hexane, 1:1). **Q** was produced in 62.5% yield (15.56 g); MS m/e 151 (M + 1); ^{1}H-NMR (CD_3OD) δ 1.08 (3H, t), 1.25–2.05 (4H, m), 2.65 (2H, t), 3.87 (5H, m), 6.89 (5H, dd, the phenolic hydrogen is hiding under the aromatic protons).

6.1.8. 1-(4-n-Butylphenoxy)-3-isopropylamino-2-propanol (**7**)

Prepared from **Q** according to the general procedures 1 and 2, chromatographed and isolated as the hydrochloride. Yield = 4.35 g, 72.1%; m.p. = 70.5–73.0 °C; MS m/e 266 (M + 1); ^{1}H-NMR (CD_3OD) δ 1.13 (3H, t), 1.75 (6H, d), 2.51–2.93 (3H, m), 3.23–3.83 (5H, bm), 4.06–4.31 (2H, m), 4.63–5.12 (2H, m), 6.77–7.28 (4H, dd). Anal. ($C_{16}H_{27}NO_2$.HCl) C, H, Cl, N.

6.1.9. 4-(n-3´-Hydroxypropyl)phenol (**T**)

Ethyl-4-hydroxyphenylpropionate (54.5 g, 250 mmol) was refluxed with benzyl bromide (44.5 g, 30.9 mL, 260 mmol), anhydrous potassium carbonate (38.7 g, 270 mmol) and sodium iodide (2.0 g) in dried acetone for 48 h. Filtration of the cooled mixture and evaporation of the solvent produced a solid residue which was taken up in ethyl acetate, washed with diluted sodium hydroxide solution and water, dried, filtered and evaporated. The product, ethyl-4-benzyloxyphenylpropionate, **R**, was purified by chromatography (silica, eluent CH_2Cl_2) and isolated as an oil. Yield = 68.6 g, 89.1%; MS m/e 309 (M + 1); ^{1}H-NMR ($CDCl_3$) δ 1.16 (3H, t), 2.76 (2H, t), 3.82 (2H, t), 4.64 (2H, q), 5.06 (2H, s), 6.88 (4H, s), 7.26 (5H, s).

Ethyl-4-benzyloxyphenylpropionate (61.6 g, 200 mmol) in anhydrous THF (200 mL) was added dropwise into a suspension of lithium aluminium hydride (8.0 g, 210 mmol) in THF (500 mL). The resultant mixture was refluxed for 2 h, cooled, the excess reagent decomposed by the dropwise addition of water and filtered. The filtrate was evaporated to dryness and the residue was purified by chromatography (silica, eluent CH_2Cl_2). The isolated product, 1-(4´-benzyloxyphenyl)-3-propanol, **S**, was recrystallised from ethanol-ether. Yield = 32.1 g, 66.2%;

m.p. = 59.5–61.5 °C; MS m/e 243 (M + 1); ^{1}H-NMR ($CDCl_3$) δ 0.72 (1H, bs), 0.87–1.23 (2H, m), 2.81 (2H, t), 3.87 (2H, t), 5.13 (2H, s), 7.11 (4H, dd), 7.52 (5H, s).

A solution of 1-(4′-benzyloxyphenyl)-3-propanol (24.2 g, 100 mmol) in ethanol (600 mL) was hydrogenated over 10% Pd/C at ambient temperature and pressure. Filtration of the catalyst and evaporation of the solvent furnished the desired phenol **T** which was purified by chromatography (silica, eluent CH_2Cl_2) and isolated as an oil. Yield = 12.81 g, 84.3%; MS m/e 153 (M + 1); ^{1}H-NMR ($CDCl_3$/CD_3OD 1:1) δ 1.77–2.23 (2H, m), 2.77 (2H, m), 3.81 (2H, m), 7.02 (4H, dd).

6.1.10. 1-(4-(n-3′-Hydroxypropyl)-phenoxy)-3-isopropylamino-2-propanol (**9**)

Prepared from **T** according to the general procedures 1 and 2, chromatographed and isolated as the hydrochloride. Yield = 2.41 g, 39.7%; m.p. = 68.5–71.5 °C; MS m/e 268 (M + 1); ^{1}H-NMR (CD_3OD) δ 1.62 (6H, d), 1.83–2.29 (2H, m), 2.61–3.12 (2H, m), 3.15–3.94 (6H, m), 4.07–4.36 (2H, m), 6.90–7.48 (4H, dd). Anal. ($C_{15}H_{25}NO_3$.HCl) C, H, Cl, N.

6.1.11. 4-n-Propoxyphenol (**F**)

n-Propyl bromide (6.8 g, 55 mmol), 4-benzyloxyphenol (10.11 g, 50 mmol), anhydrous K_2CO_3 (8.29 g, 60 mmol) and NaI (0.5 g) were stirred and heated to reflux in anhydrous acetone (250 mL) for 48 h. The solvent was evaporated and the residue was partitioned between dichloromethane and water. The organic layer was washed with water and dried over anhydrous $MgSO_4$. The solvent was evaporated and the residual 4-n-propoxyphenylbenzylether **D** (R′ = Me) was recrystallised from EtOH. Yield = 11.07 g, 83.2%; m.p. = 67–69 °C; MS m/e 243 (M + 1); ^{1}H-NMR ($CDCl_3$) δ 1.22 (3H, t), 1.70–2.23 (2H, m), 4.03 (2H, t), 5.14 (2H, s), 7.03 (5H, s), 7.52 (4H, s).

The ether **D** (R′ = Me) (10.1 g, 42 mmol) in EtOH (200 mL) was hydrogenated over 10% Pd/C (0.1 g) at room temperature and atmospheric pressure. When hydrogen absorption ceased, the reaction mixture was filtered and evaporated to dryness. The product **F** was recrystallised from EtOH. Yield = 5.12 g, 80.2%; m.p. = 67–69 °C; MS m/e 153 (M + 1); ^{1}H-NMR ($CDCl_3$) δ 1.19 (3H, t), 1.77–2.26 (2H, m), 4.06 (2H, t), 6.73 (1H, s), 6.99 (4H, s).

6.1.12. 1-(4-n-Propoxyphenoxy)-3-isopropylamino-2-propanol (**10**)

Prepared from **F** according to the general procedures 1 and 2, chromatographed and isolated as the hydrochloride. Yield = 3.56 g, 58.6%; m.p. = 116.5–119.0 °C; MS m/e 268 (M + 1); ^{1}H-NMR (CD_3OD) δ 1.22 (3H, t), 1.72 (6H, d), 1.79–2.18 (2H, m), 3.27–3.78 (4H, m), 3.87–4.29 (4H, m), 4.55–6.07 (1H, m), 5.48–5.74 (1H, m), 6.92 (4H, s). Anal. ($C_{15}H_{25}NO_3$.HCl) C, H, Cl, N.

6.1.13. 4-Cyclohexylethoxyphenol (**G**)

4-Cyclohexylethyl bromide (10.5 g, 55 mmol), 4-benzyloxyphenol (10.11 g, 50 mmol), anhydrous K_2CO_3 (8.29 g, 60 mmol) and NaI (0.5 g) were stirred and refluxed in anhydrous acetone (250 mL) for 48 h. The solvent was evaporated and the residue was partitioned between dichloromethane and water. The organic layer was washed with water and dried over anhydrous $MgSO_4$. The solvent was evaporated and the residual 4-(4′-cyclohexylethoxy)phenylbenzylether **D** (R′ = cylohexyl) was recrystallised from EtOH. Yield = 13.6 g, 81.4%; m.p. = 68–70 °C; MS m/e 311 (M + 1); ^{1}H-NMR ($CDCl_3$) δ 0.89–1.96 (13H, m), 3.65–4.02 (2H, m), 4.95 (2H, s), 6.72 (4H, s), 7.24 (5H, s).

The ether **D** (R′ = cyclohexyl) (12.0 g, 36 mmol) in EtOH (200 mL) was hydrogenated over 10% Pd/C (0.1 g) at room temperature and atmospheric pressure. When hydrogen absorption ceased, the reaction mixture was filtered and evaporated to dryness. The product **G** was recrystallised from EtOH. Yield = 7.78 g, 85.6%; m.p. = 91–93 °C; MS m/e 221 (M + 1); ^{1}H-NMR ($CDCl_3$) δ 0.77–2.01 (13H, m), 3.65–4.21 (2H, m), 4.47 (1H, s), 6.73 (4H, s).

6.1.14. 1-(4-Cyclohexylethoxyphenoxy)-3-isopropylamino-2-propanol (**15**)

Prepared from **G** according to the general procedures 1 and 2, chromatographed and isolated as the hydrochloride. Yield = 4.91 g, 66.3%; m.p. = 131.0–133.0 °C; MS m/e 336 (M + 1); ^{1}H-NMR (CD_3OD) δ 0.91 (6H, d), 0.64–1.53 (11H, bm), 2.80 (4H, m), 3.87 (5H, m), 6.43 (4H, s). Anal. ($C_{20}H_{33}NO_3$.HCl) C, H, Cl, N.

6.1.15. 4-Fluorophenethoxyphenol (**H**)

4-Fluorophenethyl bromide (11.16 g, 55 mmol), 4-benzyloxyphenol (10.11 g, 50 mmol), anhydrous K_2CO_3 (8.29 g, 60 mmol) and NaI (0.5 g) were stirred and refluxed in anhydrous acetone (250 mL) for 48 h. The solvent was evaporated and the residue was partitioned between dichloromethane and water. The organic layer was washed with water and dried over anhydrous $MgSO_4$. After evaporation of the solvent, the residual 4-(4′-fluorophenethoxy)phenylbenzylether **D** (R′ = 4-fluorophenyl) was recrystallised from EtOH. Yield = 15.2 g, 87.9%; m.p. = 113–114 °C; MS m/e 323 (M + 1); ^{1}H-NMR ($CDCl_3$) δ 3.05 (2H, m), 4.12 (2H, m), 5.11 (2H, s), 6.88 (5H, s), 7.10 (4H, dd), 7.55 (5H, dd).

The ether **D** (R′ = 4-fluorophenyl) (13.84 g, 40 mmol) in EtOH (250 mL) was hydrogenated over 10% Pd/C

(0.1 g) at room temperature and atmospheric pressure. When hydrogen absorption ceased, the reaction mixture was filtered and evaporated to dryness. The product **H** was recrystallised from toluene. Yield = 7.12 g, 76.1%; m.p. = 166–168 °C; MS m/e 233 (M + 1); ^{1}H-NMR ($CDCl_3$) δ 2.45 (2H, m), 3.56 (2H, m), 4.67 (1H, s), 6.53 (4H, dd), 6.93 (5H, dd, the phenolic hydrogen is hiding under the aromatic protons).

6.1.16. 1-(4-(4′-Fluorophenethoxy)-phenoxy)-3-isopropylamino-2-propanol (**16**)

Prepared from **H** according to the general procedure, chromatographed and isolated as the hydrochloride. Yield = 11.71 g, 61.4%; m.p. = 136.0–138.0 °C; MS m/e 348 (M + 1); ^{1}H-NMR (CD_3OD) δ 1.16 (6H, d), 2.71–3.32 (6H, m), 3.71–4.22 (4H, m), 6.46 (4H, s), 6.73 (4H, dd). Anal. ($C_{20}H_{26}FNO_3$.HCl) C, H, Cl, F, N.

6.1.17. 4-(2′-Methylpropoxy)ethoxyphenol (**M**)

2-Methylpropoxyethyl bromide (9.96 g, 55 mmol), 4-benzyloxyphenol (10.11 g, 50 mmol), anhydrous K_2CO_3 (8.29 g, 60 mmol) and NaI (0.5 g) were stirred and refluxed in anhydrous acetone (250 mL) for 48 h. The solvent was evaporated and the residue was partitioned between dichloromethane and water. The organic layer was washed with water and dried over anhydrous $MgSO_4$. The solvent was evaporated and the residual 4-(2-methylpropoxyethoxy)phenylbenzylether **L** (R′′ = 2-methylpropyl) was purified by chromatography (silica, eluent CH_2Cl_2) and isolated as an oil, homogenous by TLC. Yield = 13.8 g, 83.6%; MS m/e 301 (M + 1); ^{1}H-NMR ($CDCl_3$) δ 1.16 (6H, d), 1.87–2.35 (1H, m), 3.33–3.60 (2H, m), 3.77–4.35 (4H, m), 5.12 (2H, s), 6.94 (4H, dd), 7.52 (5H, s).

The ether **L** (R′′ = 2-methylpropyl) (10.8 g, 36 mmol) in EtOH (200 mL) was hydrogenated over 10% Pd/C (0.1 g) at room temperature and atmospheric pressure. When hydrogen absorption ceased, the reaction mixture was filtered and evaporated to dryness. The product **M** was purified by chromatography (silica, eluent CH_2Cl_2) and isolated as an oil, homogenous by TLC. Yield = 6.85 g, 86.5%; MS m/e 221 (M + 1); ^{1}H-NMR ($CDCl_3$) δ 1.18 (6H, d), 1.97–2.42 (1H, m), 3.38–3.64 (2H, m), 3.80–4.39 (4H, m), 6.96 (1H, s), 7.02 (4H, dd).

6.1.18. 1-4′-(2′′-Methylpropoxyethoxyphenoxy)-3-isopropylamino-2-propanol (**18**)

Prepared from **M** according to the general procedures 1 and 2, chromatographed and isolated as the hydrochloride. Yield = 4.00 g, 55.3%; m.p. = 89.5–91.3 °C; MS m/e 326 (M + 1); ^{1}H-NMR (CD_3OD) δ 1.13 (6H, d), 1.75 (6H, d), 3.37–3.62 (6H, bm), 3.80–4.37 (7H, bm), 6.94 (4H, s). Anal. ($C_{18}H_{31}NO_4$.HCl) C, H, Cl, N.

6.1.19. 4-(2′-Tetrahydrofurylmethoxy)ethoxyphenol (**N**)

2-Bromomethyl tetrahydrofuran (11.5 g, 55 mmol), 4-benzyloxyphenol (10.11 g, 50 mmol), anhydrous K_2CO_3 (8.29 g, 60 mmol) and NaI (0.5 g) were stirred and heated to reflux in anhydrous acetone (250 mL) for 48 h. The solvent was evaporated and the residue was partitioned between dichloromethane and water. The organic layer was washed with water and dried over anhydrous $MgSO_4$. The solvent was evaporated and the residual 4-(2′-tetrahydrofurylmethoxy)ethoxyphenylbenzyl ether **L** (R′′ = 2′-tetrahydrofurylmethyl) was purified by chromatography (silica, eluent CH_2Cl_2) and isolated as an oil, homogenous by TLC. Yield = 14.6 g, 80.9%; MS m/e 329 (M + 1); ^{1}H-NMR ($CDCl_3$) δ 1.73–2.29 (4H, m), 3.48–4.39 (9H, m), 5.12 (2H, s), 7.03 (4H, s), 7.55 (5H, s).

The ether **L** (R′′ = 2′-tetrahydrofurylmethyl) (11.8 g, 36 mmol) in EtOH (200 mL) was hydrogenated over 10% Pd/C (0.1 g) at room temperature and atmospheric pressure. When hydrogen absorption ceased, the reaction mixture was filtered and evaporated to dryness. The product **N** was purified by chromatography (silica, eluent CH_2Cl_2) and isolated as an oil, homogenous by TLC. Yield = 6.85 g, 80.1%; MS m/e 238 (M + 1); ^{1}H-NMR ($CDCl_3$) δ 1.73–2.32 (4H, m), 3.57–4.52 (9H, m), 6.81 (1H, s), 6.91 (4H, s).

6.1.20. 1-4′-(2′′-Tetrahydrofurylmethoxy)ethoxyphenoxy)-3-isopropylamino-2-propanol (**20**)

Prepared from **N** according to the general procedures 1 and 2, chromatographed and isolated as the hydrochloride. Yield = 3.59 g, 48.4%; m.p. = 165.5–167.0 °C; MS m/e 336 (M + 1); ^{1}H-NMR (CD_3OD) δ 0.93 (6H, d), 1.73–2.32 (4H, m), 2.38–3.23 (6H, bm), 3.57–4.52 (9H, m), 6.93 (4H, s). Anal. ($C_{19}H_{31}NO_5$.HCl) C, H, Cl, N.

6.1.21. 4-n-Pentyloxyethoxyphenol (**O**)

n-Pentyloxyethyl bromide (10.72 g, 55 mmol), 4-benzyloxyphenol (10.11 g, 50 mmol), anhydrous K_2CO_3 (8.29 g, 60 mmol) and NaI (0.5 g) were stirred and refluxed in anhydrous acetone (250 mL) for 48 h. The solvent was evaporated and the residue was partitioned between dichloromethane and water. The organic layer was washed with water and dried over anhydrous $MgSO_4$. The solvent was evaporated and the residual 4-(4′-n-pentyloxyethoxy)phenylbenzyl ether **L** (R′′ = n-pentyl) was purified by chromatography (silica, eluent CH_2Cl_2) and isolated as an oil, homogenous by TLC. Yield = 13.7 g, 79.4%; MS m/e 315 (M + 1); ^{1}H-NMR ($CDCl_3$) δ 1.03 (3H, t), 1.19–2.02 (8H, m), 3.53–4.22 (4H, m), 5.16 (2H, s), 6.87 (4H, s), 7.24 (5H, s).

The ether **L** (R′′ = n-pentyl) (11.3 g, 36 mmol) in EtOH (200 mL) was hydrogenated over 10% Pd/C (0.1 g) at room temperature and atmospheric pressure. When hydrogen absorption ceased, the reaction mixture was filtered and evaporated to dryness. The product **O** was purified by chromatography (silica, eluent CH_2Cl_2) and isolated as an oil, homogenous by TLC. Yield = 7.52 g, 93.25%; MS m/e 225 (M + 1); ^{1}H-NMR ($CDCl_3$) δ 1.07 (3H, t), 1.22–2.07 (8H, m), 3.57–4.29 (4H, m), 6.87 (4H, s).

6.1.22. 1-(4-n-Pentyloxyethoxyphenoxy)-3-isopropylamino-2-propanol (**22**)

Prepared from **O** according to the general procedures 1 and 2, chromatographed and isolated as the hydrochloride. Yield = 3.90 g, 52.1%; m.p. = 77.0–79.0 °C; MS m/e 340 (M + 1); ^{1}H-NMR (CD_3OD) δ 1.13 (3H, t), 1.75 (6H, d), 1.36–2.10 (8H, bm), 3.26–4.04 (6H, m), 3.86–4.28 (4H, dt), 7.03 (4H, s). Anal. ($C_{19}H_{33}NO_4$.HCl) C, H, Cl, N.

6.2. Pharmacological methods

6.2.1. Isolated tissue preparations

Studies were carried out on Sprague-Dawley rat isolated atria and tracheal rings according to our method described previously [16]. All tissues were allowed to equilibrate for 45 min with Krebs Ringer physiological salt solution; the composition of which in mmol L^{-1} was NaCl, 120; KCl, 5.6; $MgSO_4$, 1.2; $CaCl_2$, 2.5; KH_2PO_4, 1.4; $NaHCO_3$, 25; glucose 11.2 and EGTA, 0.0025.

Cumulative concentration-response curves were obtained for the non-selective β-AR agonist (-)-isoprenaline in each preparation [16]. (-)-Isoprenaline was dissolved and diluted in 1 mg mL^{-1} ascorbic acid to prevent oxidation. For the measurement of antagonist activity the appropriate agent was added to the organ bath at least 30 min after the first control concentration-response curve was completed and allowed to equilibrate for 10 min before the next concentration-response curve established. The shift in this curve to the right was calculated as a pA_2 value [39]. At least three concentrations of each antagonist were examined to verify the pA_2.

6.2.1.1. Rat isolated spontaneously beating atria

Rat hearts were removed from adult animals (200–250 g) and placed in Krebs Ringer salt solution (pH 7.4) aerated with 5% CO_2 in O_2. The atria were dissected free of the ventricles and overlying tissue and placed in a 20 mL bath maintained at 37 °C and connected to an isotonic transducer. A tension of 1 g was applied and chronotropic activity was amplified and recorded on a Grass Polygraph.

6.2.1.2. Rat isolated tracheal chains

Trachea were excised from adult rats (200–250 g), dissected free of overlying tissue and cut transversely into segments about 2 mm wide. Five segments were mounted in a 20 mL bath maintained at 37 °C at a tension of 1 g. Relaxation of the segments by (-)-isoprenaline was recorded by an isotonic transducer connected to a Grass Polygraph after tone had been established by administration of 1 μM carbachol (45 min prior to concentration-response curves).

6.3. Computational methods

6.3.1. Molecular modelling

Modelling studies were performed using the SYBYL software package (Tripos Inc., version 6.40) on a Silicon Graphics Indigo 2 UNIX Workstation. The structure of the active S-isomer of compound **1** was constructed from standard bond lengths and bond angles using the sketch routine in SYBYL. The geometry of compound **1** was fully optimised in vacuo as previous studies [19] have identified that the propanolamine side-chain of aryloxypropanolamine (AOPA) type compounds can adopt common conformations in solid, theoretical gas and solution states. Optimisation was conducted using the AM1 Hamiltonian in MOPAC (version 6.0) [48], the keywords 'PRECISE', 'ESP' and 'NOMM' were specified. The keyword ESP calculates the electrostatic potential derived atomic charges, these charges have been used since they are reported to be reliable and highly correlated with ab initio ESP charges [49, 50].

6.3.2. Molecular alignment

Compounds **2**–**25** were constructed using the minimised structure of compound **1** as a starting point. The appropriate *para*-substituent was added using the add multiple atom function in SYBYL. The structure was then optimised using the AM1 Hamiltonian in MOPAC, with the keywords 'PRECISE', 'ESP' and 'NOMM' specified, however, τ_1 was fixed at 0° or 90° (*figure 1*) and the bond, dihedral and valence angles of the AOPA core structure were fixed at the optimised values for compound **1**. Therefore, two series of compounds were created, one where $\tau_1 = 0°$ and the other where $\tau_1 = 90°$. After optimisation the compounds were superimposed over the entire *N*-isopropylphenoxypropanolamine structure (compound **1**) using the linear least squares routine within SYBYL, as shown in *figure 7*.

In addition to the optimisation and superimposition of each compound a number of other physical parameters were examined:

6.3.3. Phenyl ring charge calculations

For each compound in *table II* (**1**–**25**), the AM1 ESP charges calculated for the six phenyl ring carbon atoms were added together to obtain the parameter 'phenyl ring charge'. Various oxypropanolamine and *para*-substituent conformations (ie. different τ_1, τ_2 values, *figure 1*) were examined for their effect upon phenyl ring charge. Both τ_1 and τ_2 were varied independently in 90° steps through a full 360°, giving a total of sixteen conformers examined for each compound, and the phenyl ring charge was calculated for each conformer. The phenyl ring charge did not vary greatly between conformers and therefore the value obtained when $\tau_1 = 90°$ and $\tau_2 = 0°$ was used in this study. All sixteen phenyl ring charge values calculated for a particular compound were within ± 0.04e of the value obtained when $\tau_1 = 90°$ and $\tau_2 = 0°$.

6.3.4. LogP calculations

The logP values for the twenty five compounds were calculated using the Pallas PrologP (version 1.1) program at Swinburne University of Technology, Hawthorn, Victoria, Australia. The π values [51] for the *para*-substituents were determined by subtracting the logP of compound **1** from the compound in question and are given in *table II*.

6.3.5. Length of the para-substituent

The length was defined as the distance between the *para*-carbon of the phenyl ring and the most distant non-H atom in the *para*-substituent, hence the *para*-substituent length of compound **1** is zero (*table II*). The chain length of the *para*-substituent (R-group, *table II*) was calculated for the relaxed, fully extended low energy conformation of each molecule.

6.3.6. Flexibility of the para-substituent

A measure of the flexibility was incorporated into the QSAR analysis by assigning an integer for the number of torsion angles which affect the conformation of the *para*-substituent and is given in *table II*. For example, the flexibility of compound **4** is assigned the integer 1, as rotation of terminal methyl, hydroxyl and amine groups do not affect the conformation of the *para*-substituent.

6.3.7. Development of the CoMFA model

CoMFA [41] was performed using the QSAR option in SYBYL. Both steric and electrostatic fields were considered. The probe atom had the properties of an sp^3 carbon atom and a charge of +1.0. Cut-off values were SYBYL default values and the grid step size was 2.0 Å. For each group of compounds (ie. $\tau_1 = 0°$ or 90°) the effects of changing column filtering values (≈ 1.0–16.0 kcal/mol) were examined. The CoMFA QSAR equations were generated using the PLS algorithm using the 'leave-one-out' cross validation procedure, and the number of components with the lowest standard error of prediction value was selected as the ONC. The additional physical parameters were also included in the cross validated PLS analysis to determine whether they improved q^2. The final models, non cross-validated, for the β_1- and β_2-ARs were generated using CoMFA, the combination of additional parameters that maximised q^2 and the ONC as determined above.

Acknowledgements

The authors would like to thank Ms. Leanne Styan for her technical assistance and Dr Margaret Wong for her helpful comments. This work was supported by a grant from the National Health and Medical Research Council of Australia.

References

[1] Greenidge P.A., Pharm. Acta Helv. 68 (1994) 201–210.

[2] Lafontan M., Belan M., J. Lipid Res. 34 (1993) 1057–1091.

[3] Ostrowski J., Kjelsberg M.A., Caron M.G., Lefkowitz R.J., Ann. Rev. Pharmacol. Toxicol. 32 (1992) 167–183.

[4] Strosberg A.D., Prot. Sci. 2 (1993b) 1198–1209.

[5] Emorine L.J., Marullo S., Briend-Sutren M.M., Patey G., Tate K., Delavier-Klutchko C., Strosberg A.D., Science 245 (1989) 1118–1121.

[6] Frielle T.J., Collins S., Daniel K.W., Caron M.G., Lefkowitz R.J., Kobilka B.K., Proc. Natl. Acad. Sci. USA 84 (1987) 7920–7924.

[7] Kobilka B.K., Dixon R.A.F., Frielle T., Dohlman H.G., Bolanowski M.A., Sigal I.S. et al., Proc. Natl. Acad. Sci. USA 84 (1987) 46–50.

[8] Donne-Op Den Kelder G.M., Bultsma T., Timmerman H., Rademaker B., J. Med. Chem. 31 (1988) 1069–1079.

[9] Linschoten M.R., Bultsma T., Ijzerman A.P., Timmerman H., J. Med. Chem. 29 (1986) 278–286.

[10] Ball J.B., Nero T.L., Iakovidis D., Tung L., Jackman G., Louis W.J., J. Med. Chem. 35 (1992) 4676–4682.

[11] Baldwin J.J., Christy M.E., Denny G.H., Habecker C.N., Freedman M.B., Lyle P.A. et al., J. Med. Chem. 29 (1986) 1065–1080.

[12] Machin P.J., Hurst D.N., Bradshaw R.M., Blaber L.C., Burden D.T., J. Med. Chem. 27 (1984) 503–509.

[13] Berthold R., Louis W.J., US Patent, US 4, 425, 362, (1984).

[14] Hoefle M.L., Hastings S.G., Meyer R.F., Corey R.M., Holmes A., Stratton C.D., J. Med. Chem. 18 (1975) 148–152.

[15] Large M.S., Smith L.H., J. Med. Chem. 25 (1982) 1286–1292.

[16] Louis S.N.S., Nero T.L., Iakovidis D., Jackman G.P., Louis W.J., Eur. J. Pharmacol. 367 (1999) 431–435.

[17] Beckett A.H., Fortschr. Arzneim. Forsch. 1 (1959) 455–530.

[18] Easson L.H., Stedman E., Biochem. J. 27 (1933) 1257–1266.

[19] Nero T.L., Louis W.J., Iakovidis D., J. Mol. Struct. (Theochem.) 285 (1993) 251–272.

[20] Brandstrom A.E., Carlsson P.A.E., Carlsson S.A., Corrodi H.R., Ek L., Ablad B.A.H., US Patent, US 3928601, (1975).

[21] Carlsson P.A.E., Brandstrom A.E., Lamm B.R., Ablad B.A.H., Carlsson S.A.I., Corrodi H.R., Ek L., DE Patent, DE 2020864, (1970).

[22] Crowther A.F., Gilman D.J., McLoughlin B.J., Smith L.H., Turner R.W., Wood T.M., J. Med. Chem. 12 (1969) 638–642.

[23] Erez M., Shtacher G., Weinstock M., J. Med. Chem. 21 (1978) 982–984.

[24] Ferrari G., Ferrini R., Casagrande C., Boll. Chim. Farm. 107 (1968) 234–248.

[25] Jain P.C., Belleau B., Rastogi S.N., Anand N., Tripathi O.N., Srimal R.C., Indian J. Chem. 12 (1974) 1021–1027.

[26] Leigh T., GB Patent 1185046 (1970).

[27] Loevgren K., Hedberg A., Nilsson J., Lars G., J. Med. Chem. 24 (1981) 451–454.

[28] Machin P.J., Hurst D.N., Bradshaw R.M., Blaber L.C., Burden D.T., Fryer A.D., Melarange R.A., Shivdasani C., J. Med. Chem. 26 (1983) 1570–1576.

[29] Malguzzi R., Giordano C., EP Patent, EP 50885 (1982).

[30] Manoury P.M., Binet J.L., Rousseau J., Lefevre-Borg F.M., Cavero I.G., J. Med. Chem. 30 (1987) 1003–1011.

[31] Rosell G., Mauleon D., Pujol M.D., Granados R., Arch. Farmacol. Toxicol. (1986) 65–70.

[32] Wick A.E., Binet J., US Patent, US 4515814 (1985).

[33] Zaagsma J., Nauta W.T., J. Med. Chem. 17 (1974) 507–513.

[34] Vogel A.I., Practical Organic Chemistry 3rd ed. Longmann, London, 1962 pp. 676–962.

[35] Isagulyants V.I., Tisukova V.N., Favorskaya N.A., Oganesyan P.O., Chem. Abstracts 62 (1962) 14545a.

[36] Van Rossum J.M., Hurkmans J.A.T.M., Wolters C.J.J., Arch. Int. Pharmacodyn. Ther. 143 (1963) 299–330.

[37] Zaborowsky B.R., McMahan W.C., Griffin W.A., Norris F.H., Ruffolo Jr. R.R., J. Pharmacol. Methods 4 (1980) 165–178.

[38] MicroCal Origin, MicroCal Software Inc., USA.

[39] Mackay D.J., Pharm. Pharmacol. 30 (1978) 312–313.

[40] Baldwin J.J., Denny G.H., Hirschmann R., Freedman M.B., Ponticello G.S., Gross D.M., Sweet C.S., J. Med. Chem. 26 (1983) 950–957.

[41] Cramer R.D., Paterson D.E., Bunce J.D., J. Am. Chem. Soc. 110 (1988) 5959–5967.

[42] Triggle D.J., in: Triggle D.J., Triggle C.R. (Eds.), Chemical pharmacology of the synapse, Academic Press, London, 1976 p. 233.

[43] Belleau B., Ann. NY Acad. Sci. 139 (1967) 580–605.

[44] Dixon R.A.F., Sigal I.S., Strader C.D., Cold Spring Harbor Symposium Quant. Biology. 3 (1988) 487–497.

[45] Lewell X.Q., Drug Design Discovery 9 (1992) 29–48.

[46] Strader C.D., Candalore M.R., Hill W.S., Dixon R.A.F., Sigal I.S., J. Biol. Chem. 264 (1989) 13572–13578.

[47] Strader C.D., Sigal I.S., Register R.B., Candelore M.R., Rands E., Dixon R.A.F., Proc. Natl. Acad. Sci. USA 84 (1987) 4384–4388.

[48] Dewar M.J.S., Zoebisch E.G., Healy E.F., Stewart J.J.P., J. Am. Chem. Soc. 107 (1985) 3902–3909.

[49] Besler B.H., Merz Jr. K.M., Kollman P.A., J. Computat. Chem. 11 (1990) 431–439.

[50] Ferenczy G.G., Reynolds C.A., Richards W.G., J. Computat. Chem. 11 (1990) 159–169.

[51] Hansch C., Leo A., Unger S.H., Kim K.H., Nikaitani D., Lien E.J., J. Med. Chem. 16 (1973) 1207–1216.